Available online at www.sciencedirect.com

ScienceDirect

Procedia CIRP 71 (2018) 144–149

www.elsevier.com/locate/procedia

4th CIRP Conference on Surface Integrity (CSI 2018)

# Experimental and PFEM-simulations of residual stresses from turning tests of a cylindrical Ti-6Al-4V shaft

Jonas Holmberg[a,b]*, Juan Manuel Rodríguez Prieto[c], Johan Berglund[a], Ales Sveboda[c], Pär Jonsén[c]

[a]*Swerea IVF AB, Argongatan 30 , Mölndal SE-431 53, Sweden,* [b]*Department of Engineering Science, University West, Trollhättan SE-461 86*
[c]*Division of Mechanics of Solid Materials Department of Engineering Sciences and Mathematics. Luleå University of Technology, Luleå SE-971 87, Sweden*

* Corresponding author. Tel.: +46 70780 60 72; fax: +46 31 27 61 30. *E-mail address:* jonas.holmberg@swerea.se

**Abstract**

Alloy Ti-6Al-4V is a frequently used material in aero space applications due the high strength and low weight. This material is however often considered as a difficult to machine alloy due to several material properties such as the inherent characteristics of high hot hardness and strength which is causing an increased deformation of the cutting tool during machining. The thermal properties also cause a low thermal diffusion from locally high temperatures in the cutting zone that allows for reaction to the tool material resulting in increased tool wear.
Predicting the behavior of machining of this alloy is therefore essential when selecting machining tools or machining strategies. If the surface integrity is predicted, the influence of different machining parameters could be studied using Particle Finite Element (PFEM)-simulations. In this investigation the influence from cutting speed and feed during turning on the residual stresses has been measured using x-ray diffraction and compared to PFEM-simulations.
The results showed that cutting speed and feed have great impact on the residual stress state. The measured cutting force showed a strong correlation especially to the cutting feed. The microstructure, observed in SEM, showed highly deformed grains at the surface from the impact of the turning operation and the full width half maximum from the XDR measurements distinguish a clear impact from different cutting speed and feed which differed most for the higher feed rate.
The experimental measurements of the residual stresses and the PFEM simulations did however not correlate. The surface stresses as well as the sign of the residuals stresses differed which might be due to the material model used and the assumption of using a Coulomb friction model that might not represent the cutting conditions in the investigated case.


Selection and peer-review under responsibility of the scientific committee of the 4th CIRP Conference on Surface Integrity (CSI 2018).

*Keywords:* Ti-6Al-4V, X-ray diffraction, PFEM

## 1. Introduction

The alloy Ti-6Al-4V is frequently used in aero space engine applications mainly due to its properties of low weight in relation to the high strength at elevated temperatures [1].

However, this alloy is often considered as a difficult to machine alloy due to the inherent characteristics from the hot strength which is causing increased wear and deformation of the cutting tool during machining. This is mainly due to the low thermal conductivity in combination with the material's reactivity to other materials which with the high temperatures in the cutting zone cause a strong adhesion to the work piece material [2]. Further, machining of this alloy is often associated with relatively low cutting speeds due to the increased risk of rapid chipping and plastic deformation of the tool edge [3]. This risk will further increase when the tool wears out and the high dynamic shear strength increase results in localized shear stress and development of saw-tooth chips. This chip formation in combination with the material's low modulus of elasticity will also result in vibrations during machining increasing the risk of notching the cutting tool [4].

A rather small process window, cutting speeds typically less than 60 m/min and feed less than 0.25 mm/rev, are often selected in order to control the chip formation and avoid


Selection and peer-review under responsibility of the scientific committee of the 4th CIRP Conference on Surface Integrity (CSI 2018).
10.1016/j.procir.2018.05.087

serrated chips [5-6]. However, for productivity reasons it is of great interest to investigate higher cutting speeds which then need to be verified regarding the resulting work piece surfaces.

The resulting residual stress state of the machined surface is essential to verify and attempts has been made to predict this using simulations [7-8]. Özel et al. presented a FE simulation to predict this which was based on a good material model [8]. These results showed that FE simulations could be used to describe the cutting process quite well. If the surface integrity can be predicted, the influence of different machining parameters could be studied using relatively fast FE-simulations. Lately, also simulations with Particle Finite Element Methods (PFEM) has been shown to describe the cutting process well in terms of chip formation, cutting force and heat exchange in the cutting zone by Rodríguez et al. [9]. PFEM simulation is a method based on a collection of particles given velocity, transporting momentum and physical properties such as position, displacement, strain, stress etc. In the PFEM simulation this collection of particles moves in a Lagrangian manner accordingly. PFEM in metal cutting has further been described by Rodríguez et al. [10]. However, even though PFEM has been employed to explore the cutting process still no report has been made where the actual resulting residual stress state has been simulated which is one of the objectives with the present investigation. The limited published results on how the work piece surface integrity has been affected by cutting parameters from turning in Ti-6Al-4V in combination with an attempt to predict the residual stresses using PFEM has motivated the present work.

In this investigation the influence from cutting speed and feed during turning has been studied with the objective to clarify the impact on the residual stresses and to explore how well PFEM could assess the residual stress state of the machined surface.

## 2. Material and experimental details

### *2.1. Material*

Table 1. Chemical composition of test sample bar.

| Element | Ti | Al | V | O | C | N | H | Fe | Others |
|---|---|---|---|---|---|---|---|---|---|
| [wt-%] | 89.8 | 5.7 | 4.1 | 0.15 | 0.01 | 0.01 | 0.014 | 0.15 | <0.1 |

Table 2. Material properties of test sample bar.

| Property | Value | Unit |
|---|---|---|
| Density | 4.428 | g/cm$^3$ |
| Young's modulus | 114 | GPa |
| Poisson's ratio | 0.32 | |
| Tensile strength | 960 | MPa |
| 0.2 % Yield strength | 888 | MPa |
| Elongation | 15 | % |
| Beta transus temperature | 991.5 | °C |

The tests in this investigation were performed on a forged Ti-6Al-4V cylindrical test bar with an initial diameter of 140 mm. The test bar was manufactured by hot forging followed by subsequent heat treatment (710°C in 2 h and then air cooling), straightening and rough turning. The material properties and chemical composition of the test bar is presented in Tables 1 and 2.

### *2.2. Experimental*

The turning tests were performed in a George Fischer CNC lathe, by orthogonal turning using triangular inserts to cut the test bar at six different positions, race tracks (RT), according to Figure 1. Slots between the RT were cut using a parting tool before the test. The dimensions of the RT were selected for an engagement of the tool over the complete surface to be cut which corresponded to a width of 4 mm. The tests were carried using radial feed and when the final depth was reached a rapid retraction of the tool was employed. The test matrix was designed to evaluate different cutting speeds (Vc) and feeds (f) shown in Figure 1. The insert tool used for the test is specified according to Table 3. Further, the cutting forces were measured using a three component Kistler dynamometer type 9263 with a 300 Hz low pass filter employed.

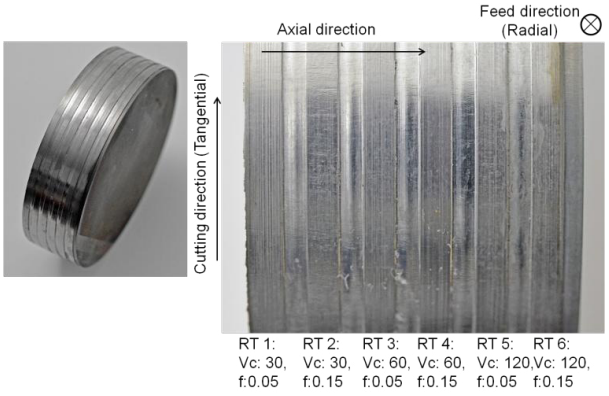


Fig 1. Overview of the test sample illustrating the different race tracks with different cutting speeds (Vc) and feeds (f).

Table 3. Properties of the cutting tool used for the turning test.

| Property | Setting | Unit |
|---|---|---|
| Tool geometry | Triangular | |
| Tool ID | TNMG 160408-QF grade 4015 | |
| Insert coating | TiCN-$Al_2O_3$ | |
| Wedge angle | 90 | ° |
| Edge radius | 47 | µm |
| Edge primary land | 0.15 | mm |
| Rake face angle | -6 | ° |

### *2.3. Examination methods*

The residual stresses were measured using X-ray diffraction with an equipment from Stresstech, XStress 3000 G2R. This diffractometer was equipped with a Titanium X-ray tube (λ:0.27497 nm) at 30kV and 6.7 mA. The lattice plane (110) was measured which has a 2θ diffraction peak located at approximately 139°. The modified $\sin^2\psi$ measurement strategy was used with 5 psi angles (40°...-40°). The residual stress was calculated assuming elastic strain theory according to Hook's law using 114 GPa as Young's modulus and 0.32 as Poisson's ratio, further described by

Noyan and Cohen [11]. Measurements of residual stress profiles were performed with layer removal where successive material removal was performed by electro polishing. The electro polishing was done with Struers Movipol and Struers electrolyte A2. All measurements were performed in an accredited laboratory in accordance with the SS-EN 15304:2008 standard that describes how residual stress measurements are performed by X-ray diffraction [12].

The impact upon the microstructure was studied on polished cross sections made in cutting direction of the test bar. The polished cross sections were further prepared by etching using Kroll's reagent (100 ml $H_2O$ + 2 ml HF + 5 ml $HNO_3$) for 5-15 s. The microstructure was investigated using a Jeol 6610LV SEM and the hardness was measured with a Qness micro hardness tester and the Knoop method was employed with 100 g load which gave an appropriate sensitivity of the measurement.

### *2.4 PFEM simulations*

The numerical simulations were carried out using the Particle Finite Element Method (PFEM) developed by the authors, see Rodríguez et al. [9-10]. An orthogonal cutting operation was employed to mimic 2D plain strain conditions (see Figure 2). The depth of cut, used for all the test cases, was equal to 1 mm. The dimension of the workpiece was 8 × 1.6 mm. A horizontal velocity corresponding to the cutting speed was applied to the particles at the right side of the tool as is given in Table 3. The particles along the bottom and the left sides of the workpiece were fixed. The workpiece material was modeled using a Johnson-Cook constitutive model (see Table 4). The calibration was accomplished via a parameter fitting procedure in conjunction with material data based on uniaxial compression tests at low and high strain rates, at high strain rates a SHPB rig was used (see more information Rodríguez et al. [9]). Material properties of the tool were assumed as thermoelastic.

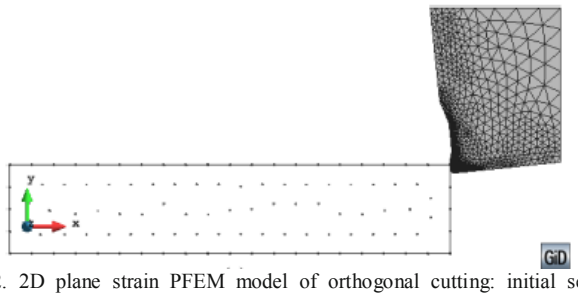


Fig 2. 2D plane strain PFEM model of orthogonal cutting: initial set of particles.

Table 4. Johnson Cook material parameters

| A [MPa] | B [MPa] | N | C | M | E_ref |
|---|---|---|---|---|---|
| 860 | 612 | 0.78 | 0.08 | 0.66 | 1 |

## 3. Results and analyses

### *3.1. Cutting force*

The cutting forces were measured in radial (feed) direction and tangential (cutting) direction. The results are presented in Table 5 which represents the average values taken when the measured signal was stable at the end of the cutting cycle. The results show that the tangential cutting force is higher than the radial force when the feed is high while for the low feed the radial feed force is higher than the tangential cutting force. Further, it could be seen that the force in feed direction is low for all combinations of cutting speed and feed.

Table 5. Results of the force measurements during the turning tests.

| Vc [m/min] | f [mm] | $F_{feed}$ [N] | $F_{cutting}$ [N] |
|---|---|---|---|
| 30 | 0.05 | 481.1 | 417.8 |
| 30 | 0.15 | 828.7 | 961.7 |
| 60 | 0.05 | 447.2 | 395.1 |
| 60 | 0.15 | 698.2 | 868 |
| 120 | 0.05 | 662.4 | 458.9 |
| 120 | 0.15 | 702.6 | 839.2 |

### *3.2. Residual stress*

The surface residual stresses and the cutting forces are shown in Figure 3. These results show a clear influence from the cutting parameters on the measured surface residual stress state and cutting forces. The residual stresses show quite high tensile stresses for Vc30/f:0.15, Vc60/f:0.05 and Vc60/f:0.15. Cutting speed 120 show similar tensile stresses independently of the feed. However, for Vc30/f:0.05 the surface stresses are instead in compression both in axial and cutting direction.

The influence of the feed on the surface residual stresses show that the feed increase the tensile residual stresses in all cases except Vc 30 in cutting direction.

The influence of the cutting speed show that low cutting speed generates compressive residual stresses while Vc 60 generates the highest tensile surface residual stress while 120 only generates moderate tensile stresses.

The measured forces correlates well with the feed which show that higher feed, 0.15, result in an approximately 50% increase of the cutting force. The influence of the cutting speed is less pronounced for low feed while for the feed of 0.15 the cutting force decays with higher cutting speed.

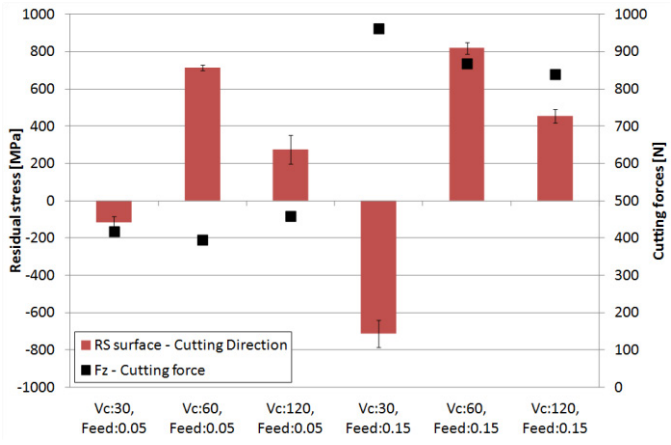


Fig. 3. Surface residual stresses and cutting forces for turning test samples.

These results clearly show that the feed has a strong influence on the resulting cutting force. However, the

influence of cutting parameters is not that obvious on the surface residual stress state which instead shows that Vc 60 has the most detrimental characteristics with high tensile residual stresses.

The results from the residual stress profile measurements are presented in Figure 4 for the cutting direction and in Figure 5 for the axial direction. These profiles show great impact from both the cutting speed and feed.

The cutting speed seems to be the most influential on the residual stress profiles in the cutting direction. For Vc 30, both for feed 0.05 and 0.15, show compressive residual stress profiles while all other profiles are tensile, seen in Figure 4. It could further be observed that Vc 60 generated the highest tensile stress profile. Similar results regarding the influence of Vc could be observed for the axial direction but the difference in magnitude between different Vc is much lower. This is characterized by that Vc 60 show the highest tensile stress followed by Vc 120 while Vc 30 show a compressive stress profile instead.

The influence of the feed is also most influential for Vc 30 which shows a much higher compressive residual stress state for 0.15 feed compared to the 0.05 feed. The results further show that Vc 60 generates the highest tensile stresses and that the feed mainly influence the penetration depth resulting in a shift of the profile of approximately 20 µm between feed 0.05 and 0.15. On the contrary, Vc 120 shows a shift of the profile towards the surface at higher feed but the magnitude of these profiles differs some.

The influence of the feed on the residual stress profiles in axial direction show less influence from the cutting parameters compared to the cutting direction. Further, feed show minor influence at low cutting speed. For Vc 60 and 120 the feed mainly influence the depth impact which shifts the profile close to the surface for Vc 60.

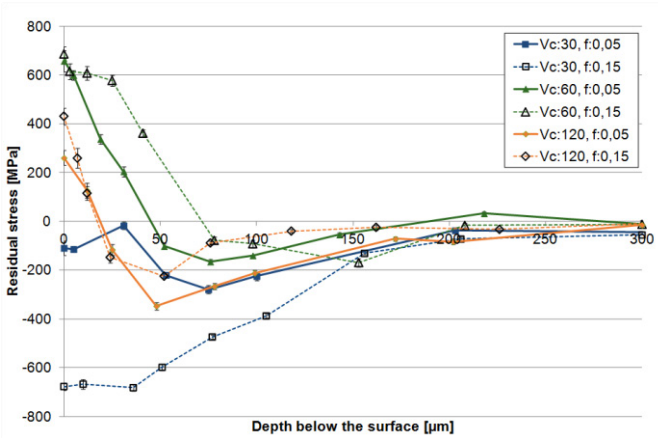


Fig. 4. Residual stress profiles, turning test samples in **cutting** direction.

Generally the profiles for Vc 60 and 120 are highly unwanted from a fatigue perspective. This shows that an additional finishing operation is required to ensure that the surface attained has compressive residual stresses. The great difference in residual stress profiles further show that there are a crossing point in the retrieved data where the Vc change from the compressive state into a tensile state. This crossing point is located in the interval of Vc 30-60 m/min.

These results show similar trends as reported by Velásquez et al. who also showed that low cutting speed resulted in compressive stresses while high cutting speed instead resulted in tensile stresses [13]. However, the magnitude of the stresses measured in this investigation is higher which could be due to a different cutting tool geometry used in this case.

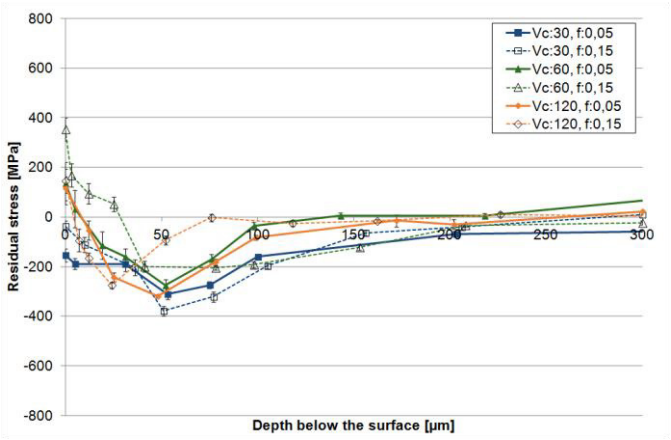


Fig. 5. Residual stress profiles, turning test samples in **axial** direction.

### *3.3. Deformation*

The diffraction peak width, full width half maximum FWHM, holds information of the deformation of the surface which is frequently used in order to evaluate the amount of cold working from e.g. shot peening [14]. The FWHM data from the performed diffraction measurements show that the surfaces have been affected to a depth of 50-200 µm depending on the machining parameters used. The results are presented in Figure 6.

These results show that with a feed of 0.05 the profiles are very similar and characterized by an impact depth of approximately 150 µm. However, for the very outer surface the Vc 60 surface indicate the highest amount of deformation. The results for feed 0.15 show greater influence from the cutting speed where Vc 60 again show the highest degree of deformation at the surface while Vc 120 show much lower impact compared to all other samples with a penetration depth of only approximately 50 µm. Both Vc 30 and Vc 60 show much deeper impact to depths of approximately 200 µm.

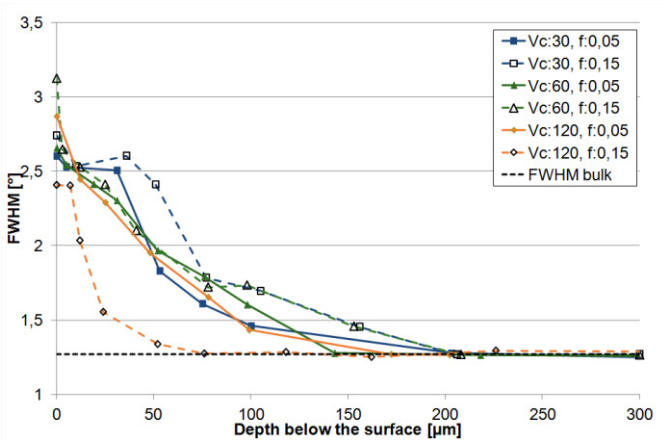


Fig. 6. The average FWHM profiles from diffraction data of the samples.

The deformation was also studied using Knoop hardness measurements, presented in Figure 7. The results showed a variation between individual indents in the profile for the different samples. The surface measurements showed a lower hardness to a depth of 50 µm for all samples. Further, a difference could be observed for the samples with a higher feed rate which showed a higher hardness in the interval from the surface and to a depth of 400 µm, especially for Vc 30.

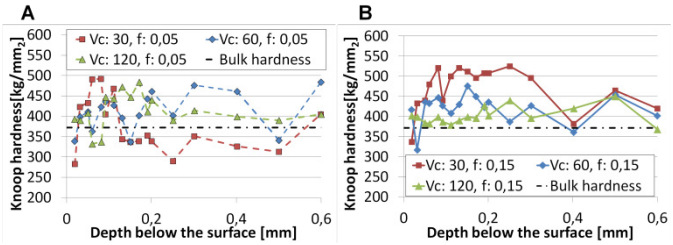


Fig.7. Hardness profiles for the samples with A: feed 0.05 and B: feed 0.15.

The microstructure was further investigated for all samples using SEM, presented in Figure 8. The surface deformations are clearly shown as sheared grains and grain boundaries in the surface. The affected depth is further illustrated by yellow lines in Figure 8. The grains are generally affected 5-15 µm below the surface for the different samples, depending on different locations across the cut surface.

Further investigations using advanced microscopy, Electron Back Scattering Diffraction, might distinguish individual differences even better between the samples.

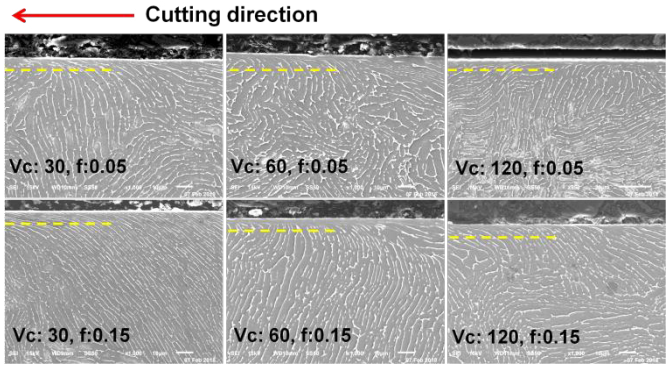


Fig. 8. Micrograph from SEM in x1000 magnification showing the impact on the surface for the different turning settings. The scale bar is 10 µm.

### *3.4. PFEM simulations*

Results from the PFEM simulations have been compared to the XRD measurements for the samples with feed 0.15 mm and Vc:30 in Figure 9, Vc:60 in Figure 10 and Vc:120 in Figure 11. The results show a great difference between the simulations and the measurements both in regard to the surface state as well as the affected depth. The PFEM predicts tensile surface residual stress state for all samples while the measurements for the Vc 30 sample show a quite high compressive residual stress state. The PFEM further show an unexpected behaviour of a fairly low surface stress state that increases with a maximal tensile stress peak located at depth of approximately 100 µm. This was not observed in the measured data. However, for some of the samples the depth position of the maximal tensile peak in the simulations coincides with the position for the measured maximal compressive stress from the measurements. The attribute that correlates quite well is the depth to which the cutting process has affected the stresses, i.e. where the residual stresses level out towards zero.

The main reason for the differences between the simuations and the measured results is believed to be due to the material model used for the PFEM simulations. This model is a simple constitutive model (Johnson-Cook) that might not be representative for the present case. A further development of the model is required where the dislocation density and a damage model need to be considered. Also, further attention to the friction needs to be considered with a model that is not based on Coulomb friction. It should also be noted that the model used for the PFEM simulation was developed in order to study the thermo-mechanical aspects of the cutting process in order to study the thermal impact and the chip formation when cutting at different speeds and feeds. Consequently, the model needs further development in order to predict residual stresses more accurately. Similar difficulties of simulating the residual stresses have been presented by Attanasio et al. [15]. They showed results where the experimental data showed high tensile stresses in the surface while the simulations showed high compressive stresses for orthogonal cutting in a carbon steel.

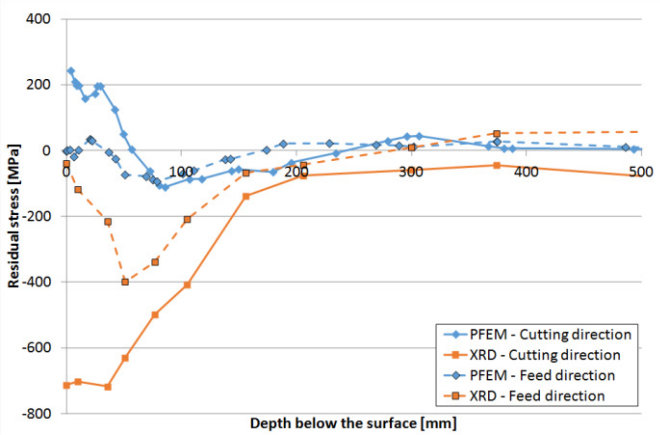


Fig.9. Residual stress profile comparison between PFEM simulations and XRD profile measurements for sample with **Vc 30** and **feed 0.15**.

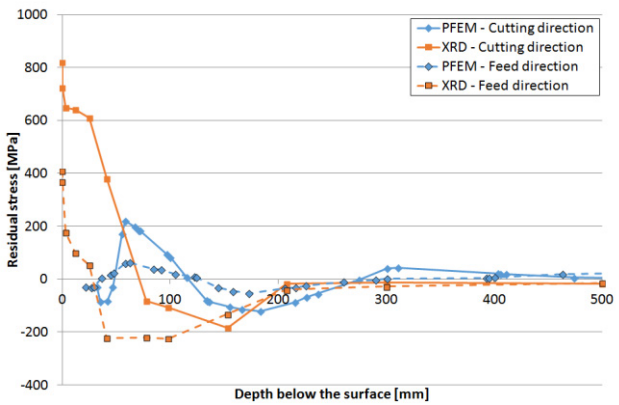


Fig.10. Residual stress profile comparison between PFEM simulations and XRD profile measurements for sample with **Vc 60** and **feed 0.15**.

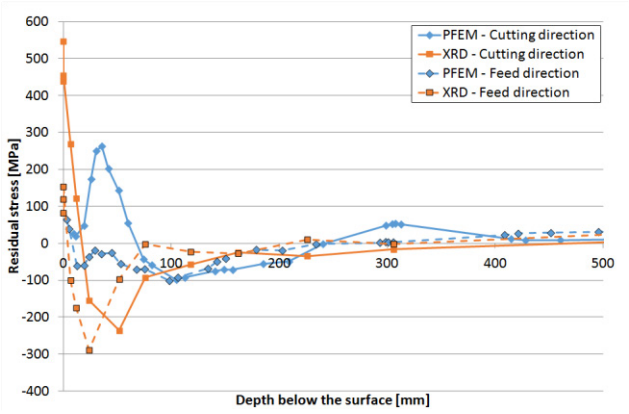


Fig.11. Residual stress profile comparison between PFEM simulations and XRD profile measurements for sample with **Vc 120** and **feed 0.15**.

## 4. Discussion

The turning operation results in plastic deformation of the surface. This is thermo-mechanically induced where the cutting parameters determine which regime that dominates. The results in this investigation showed that the thermal regime has greatest impact for high Vc while for low Vc the mechanical deformation increase. It was further observed that the highest Vc of 120 resulted in a lower tensile stress compared to Vc 60. This indicates that there exists a crossing point where the thermal impact is influencing more.

The surprisingly high compressive stresses for Vc 30 at feed 0.15 was measured and verified at two different positions with a separation of 90° on the sample showing same levels of stress throughout the profile. It could further be concluded that similar trends has been reported by Velásquez et al. [13].

## 5. Conclusions

This investigation has shown that cutting speed and feed have great impact on the cutting forces and the residual stress state. The impact from the turning operation is greatest in the cutting direction.

Increasing turning feed increases the surface tensile residual stresses in all cases in cutting direction, except for Vc 30. It has further been shown that the cutting speed has a strong impact where Vc 30 produced high compressive residual stress profiles for a feed of 0.15. For Vc 60 and 120 the profiles were tensile instead to a relatively high magnitude in the surface region, especially for Vc 60.

The cutting forces showed a clear correlation to the feed where a higher feed resulted in 50% higher cutting forces.

The FWHM showed a high impact in the surface for all samples indicating surface deformations extended to depths of 150 µm for samples with a feed of 0.05 and to depths of 50-200 µm for the samples with a feed of 0.15.

The microstructure showed a distinct impact from the cutting operation with a highly deformed surface which was also seen in the lower hardness in the surface region.

Stresses from the PFEM simulations did not show a correlation to the measured residual stresses due to limitations in the used material model.

## Acknowledgements

The authors would like to acknowledge VINNOVA for financing the project VirtFab (ref. no. 2014-00919), Sandvik, Swerea IVF, Luleå University, KK-foundation, University West and the SiCoMap research school for support.

## References

[1] Boyer RR. An overview on the use of titanium in the aerospace industry. Mater Sci Eng A 1996;213:103-114.
[2] Narutaki N, Murakoshi A, Motonishi S, Takeyama H. Study on Machining of Titanium Alloys. CIRP Ann-Manuf Techn.32;1983:65-69.
[3] Che-Haron C. Tool life and surface integrity in turning titanium alloy. J Mater Process Tech 2001;118:231–237.
[4] Cedergren S, Frangoudis C, Archenti A. Influence of work material microstructure on vibrations when machining cast Ti-6Al-4V. Int J Adv Manuf Tech 2016;84:2277–2291
[5] Dandekar CR, Shin YC, Barnes J. Machinability improvement of titanium alloy (Ti–6Al–4V) via LAM and hybrid machining. Int J Mach Tool Manu 2010;50:174–182.
[6] Ezugwu EO, Wang ZM. Titanium alloys and their machinability—a review. J Mater Process Tech 1997;68:262–274.
[7] Ulutab D, Sima M, Özel T. Prediction of Machining Induced Surface Integrity Using Elastic-Viscoplastic Simulations and Temperature-Dependent Flow Softening Material Models in Titanium and Nickel-Based Alloys. Adv Mater Res 2011;223:401–410.
[8] Özel T, Ulutan D. Prediction of machining induced residual stresses in turning of titanium and nickel based alloys with experiments and finite element simulations. CIRP Ann – Manuf Techn 2012;61: 547–550.
[9] Rodríguez J, Jonsén P, Svoboda A. Simulation of metal cutting using the particle finite-element method and a physically based plasticity model. Computuational Particle Mechanics 2017;4:35-51.
[10] Rodríguez J, Arrazola P, Cante J, Kortabarria A, Oliver J. A Sensibility Analysis to Geometric and Cutting Conditions Using the Particle Finite Element Method (PFEM). Procedia CIRP 2013;8:105-110.
[11] Noyan IC, Cohen JB. Residual Stress – Measuremenst by diffraction and interpretation. 1st ed. New York: Springer-Verlag; 1987.
[12] Eurpoeran Committee for standardization. EN-15305:2008:E Non-destructive Testing - Test Method for Residual Stress analysis by X-ray Diffraction. 2008.
[13] Puerta Velásquez JD, Tidu A, Bolle B, Chevrier P, Fundenberger JJ. Sub-surface and surface analysis of high speed machined Ti-6Al-4V alloy. Mat Sci Eng A 2010;527:2572-2578.
[14] Mathlock BS, Snoha DJ, Grendahl SM. Using XRD elastic and plastic strain data to evaluate the effectiveness of different cold-working techniques in aerospace materials. Powder Diffr 2009;24: 51-58.
[15] Attanasion A, Ceretti E, Cappellini C, Giardini C. Residual stress prediction by means of 3D FEM simulation. Adv Mater Res 2011;223:431-438.